Structure of the Acetylene−Magnesium Binary Complex from Infrared Laser Spectroscopy in Helium Nanodroplets†

D. T. Moore‡ and R. E. Miller*

Department of Chemistry, University of North Carolina, Chapel Hill, North Carolina 27599

Received: April 29, 2004; In Final Form: August 2, 2004

High-resolution infrared laser spectroscopy is used to study acetylene−magnesium complexes formed in helium nanodroplets. The rotational fine structure observed in the spectrum of the binary complex is well described by a gas-phase Hamiltonian and is used to determine that the structure is T-shaped, with the magnesium binding weakly to the triple bond of the acetylene. The binary complex has a dipole moment of 0.39 ± 5, as measured by Stark spectroscopy. Difference electron density maps reported herein reveal that this dipole moment arises from a strong polarization of the magnesium charge cloud by the quadrupole moment of the acetylene. Preliminary spectra are also reported for acetylene−Mg_n ($n = 2, 3$). Although these are not fully rotationally resolved, comparisons with ab initio calculations reported here provide some insights into the nature of these complexes.

Introduction

The interactions between adsorbate molecules and metal surfaces and particles are of fundamental interest in heterogeneous catalysis[1] and continue to be the subject of intensive research.[2] Vibrational spectroscopy of the adsorbed molecule is particularly revealing, given that the associated vibrational frequencies are strongly dependent upon the nature of the interactions with the cluster or surface.[3] Experimental techniques including reflectance−absorbance infrared spectroscopy (RAIRS)[4] and high-resolution electron energy loss spectroscopy (HREELS)[5] often have sufficient sensitivity to permit the spectroscopic detection of submonolayer coverages of molecules that are either physisorbed or chemisorbed to a metal surface. Physisorbed molecules are only weakly perturbed by the surface, while chemisorbed molecules often show significant structural distortion, with corresponding large changes in their vibrational spectra.

Consider, for example, the interactions between acetylene and a single-crystal Cu(111) surface. Experimental HREELS spectra indicate that the acetylene is bent significantly on the surface, indicative of substantial charge transfer between the surface and the molecule, causing significant rehybridization of the latter.[6,7] In contrast, matrix electron spin resonance (ESR) data suggest that the interactions of acetylene with individual copper atoms are quite weak, corresponding to a π-bonded binary complex.[8,9] Although this fundamental difference in the interactions between a single atom and the corresponding bulk metal is not unexpected, direct experimental data probing the size-dependent structural trends is still lacking.

In a series of recent papers,[10−13] we have reported high-resolution infrared spectra for a number of polar molecules, namely, hydrogen cyanide (HCN) and cyanoacetylene (HCCCN), bound to magnesium clusters of varying size. The clusters are grown in helium droplets and are thus cooled to 0.37 K.[14,15] By varying the metal vapor pressure in the pickup oven, used to dope the helium droplets, the average metal cluster size is easily controlled. Vibrational frequency shifts for the C−H stretches of the adsorbed molecules have been measured as a function of cluster size, revealing strongly nonadditive effects. In addition, rotational fine structure was observed in these spectra, providing detailed information on the associated molecular geometries. Stark spectra were also measured for these adsorbate−metal cluster systems in order to measure the corresponding dipole moments. For the HCN−Mg_4 cluster, a sudden increase in the dipole moment was observed for the $n = 4$ complex, which we attribute to the onset of charge transfer between the molecule and the magnesium complex.[12]

In the present study, we report our first studies of a nonpolar molecule (acetylene) bound to magnesium clusters. The spectrum of the binary complex is rotationally resolved and provides conclusive evidence for a "T-shaped" structure, with the magnesium atom bound to the π cloud of the acetylene. This is in excellent agreement with ab initio calculations that are also reported here. Using Stark spectroscopy, we also measured the dipole moment of this binary complex, which is mainly attributed to the interaction between the quadrupole moment of the acetylene and the large polarizability of the magnesium atom. Preliminary vibrational spectra and ab initio calculations are also presented for acetylene−Mg_n ($n = 2, 3$).

In an earlier, laser-ablation matrix-isolation study of the acetylene−magnesium system, only reaction products were reported, while the weakly bound complexes studied here were not observed.[16] This difference is most likely due to the fact that helium droplets provide an efficient medium for removing the condensation energy released during complex formation, stabilizing the initial van der Waals complexes and inhibiting further reaction.[17,18]

Experimental Methods

The helium droplet apparatus used in the present study has been discussed in detail previously.[19,20] Helium droplets are produced by expanding ultrapure (99.9999%) helium at high pressure (60−70 bar) through a 5 μm diameter nozzle, cooled

† Part of the special issue "Tomas Baer Festschrift".

‡ Current address: FOM Institute for Plasma Physics Rijnhuizen, 3439 MN Nieuwegein, The Netherlands.

10.1021/jp0403238 CCC: $27.50
Published on Web 10/20/2004

by a closed-cycle helium refrigerator. In the present experiments, the nozzle temperature was held at ∼20 K, resulting in a beam with a mean droplet size of several thousand helium atoms. Mg atoms are introduced by passing the droplet beam through a 1.3 cm long magnesium oven, consisting of a closed copper tube heated by a 225 W cartridge heater (Omega). Magnesium pellets (Aldrich) are placed in the oven, which is then heated to an operating temperature of ∼300 °C, such that the vapor pressure of the magnesium was sufficient to dope the droplets with one or more atoms.

To avoid the complications associated with the well-known Fermi resonance in the ν_3 band of acetylene,[21] we used $^{13}C_2H_2$ (99%, Cambridge Isotope Laboratories), which was introduced into a separate pickup cell located downstream of the magnesium oven. The acetylene pressure was maintained at $\sim 10^{-6}$ Torr (uncorrected ion gauge reading) to optimize for the pickup of a single acetylene molecule.

After being doped with the species of interest, the droplets pass through a parallel multipass cell, used to repeatedly reflect the infrared laser across the droplet beam path, significantly increasing the excitation efficiency. The tunable infrared light was provided by a color-center laser (Burleigh, crystal no. 3), pumped by a Kr-ion laser (SpectraPhysics). Details concerning the tuning and calibration of the laser system can be found elsewhere.[22] Electrodes have been placed on either side of the laser interaction region, so that a large dc electric field (up to ∼ 40 kV/cm) can be applied for the measurement of Stark spectra for determination of dipole moments. The wavelength-dependent depletion of the droplet beam is monitored using a liquid-He-cooled bolometer (Infrared Laboratories), operating at ∼1.4 K. This depletion results from the relaxation of the excited vibrational state of the acetylene (the ν_3 mode of ^{13}C acetylene at ∼3380 cm^{-1}) to the liquid helium. Given that the binding energy of a helium atom to the droplet is quite small (∼5 cm^{-1}),[15] vibrational relaxation results in the evaporation of several hundred helium atoms. Amplitude modulation of the laser and phase-sensitive detection of the bolometer signal then provide background-free spectra.

Ab Initio Calculations

Geometry optimizations were performed for several different isomers of the acetylene−Mg and acetylene−Mg_2 complexes, using the BCCD(T) and MP2 methods and the 6-311++G-(3df,3pd) basis set. Vibrational frequencies for optimized structures were also calculated at the MP2 level. Unless otherwise noted, all structures represent stable minima with no imaginary frequencies. All reported binding energies have been counterpoise corrected for basis set superposition error in the usual way,[23] using reference monomers calculated in the presence of all basis functions of the corresponding complex. Dipole moments reported for the BCCD(T) calculations were computed from the Brueckner reference densities according to the Brueckner orbital expectation value (BOX) scheme of Hesselmann and Jansen.[24] An unrelaxed, counterpoise corrected potential energy surface (PES) was also computed for the HCCH−Mg binary complex, by scanning over the intermolecular Jacobi coordinates, shown as an inset in Figure 1. A total of 84 points were calculated, at 12 values of R (3.25, 3.5, 3.75, 4.0, 4.25, 4.5, 4.75 5.0, 5.5, 6.0, 6.5, and 7.5 Å), and 7 angles, corresponding to the (positive) 10-point Legendre angles,[25] as well as 0° and 90°. The resulting BCCD(T)/6-311++G(3df, 3pd) PES is plotted in Cartesian coordinates in Figure 1, revealing the global minimum in the T-shaped geometry and a shallow, secondary minimum in the linear configuration.

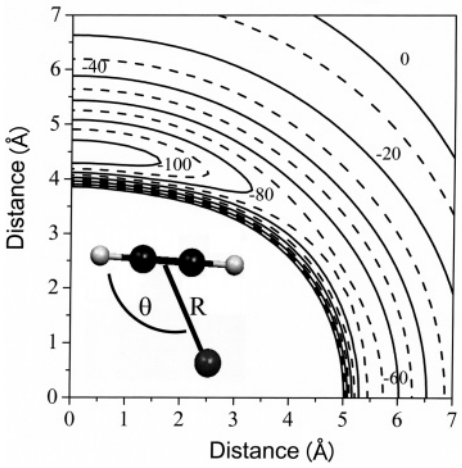

Figure 1. A potential energy surface calculated for the acetylene−Mg binary complex at the BCCD(T)/6-31++G(3df,3pd) level. The contour spacing is 10 cm^{-1}, with even (odd) multiples of 10 represented as solid (dashed) lines. The global minimum is in the T-shaped geometry at −106 cm^{-1}. The inset shows the Jacobi coordinates used for scanning the intermolecular potential energy surface.

Full geometry optimizations and (MP2) frequency calculations were carried out for both the T-shaped and linear configurations, and the resulting structural parameters and asymmetric CH stretching frequencies are summarized in Table 1, along with the corresponding data for the acetylene monomer (obtained at the same level of theory). As expected for weakly bound systems, the formation of the complexes does not appreciably distort the acetylene molecule. The calculated vibrational frequency shift of the asymmetric CH stretch for the T-shaped complex (relative to free acetylene) is calculated to be 1.68 cm^{-1}. BCCD(T) [MP2] binding energies for the T-shaped and linear geometries are 105 [135] cm^{-1} and 72 [101] cm^{-1}, respectively (Table 1).

Difference densities (sometimes called deformation densities[26]) were also computed for the HCCH−Mg and HCCH−Mg_2 complexes by subtracting the counterpoise corrected electron densities of the fragments from the electron density of the full complex. The difference density maps were constructed using the Brueckner reference densities (calculated at the BCCD-(T) optimized geometry of the complex) as per the BOX scheme.[24] The MOLPRO 2000.3 computational chemistry package[27] was used for all of the calculations reported herein.

Results: Binary Complex

Figure 2 shows two spectra recorded in the region of the asymmetric C−H stretching band (ν_3) of $^{13}C_2H_2$, using a coarse laser tuning method (300 MHz per step). The spectrum in Figure 2a was recorded with the magnesium oven at room temperature and shows transitions associated with acetylene monomer in helium,[21] as well as a band assigned to the acetylene dimer. When the magnesium oven temperature is increased to ∼300 °C, three new bands appear in the spectrum, as shown in Figure 2b. The oven temperature needed to optimize the new bands is consistent with that for the pickup of a single magnesium atom, based upon our previous work on HCN−Mg,[10,11] thus providing us with an initial assignment of these bands to the binary acetylene−Mg complex. Given that the spacings between these three bands are similar to those in the monomer spectrum, the suggested assignment is to perpendicular sub-bands of a T-shaped, near-prolate top with C_{2v} symmetry. Indeed, the quantum numbers given in the figure are based upon this

TABLE 1: Results of Ab Initio Geometry Optimizations and Frequency Calculations (6311++G(3df,3pd) Basis) for Two Isomers of the Mg−Acetylene Complex[a]. The Results for the Acetylene Monomer ($^{13}C_2H_2$) are Also Given for the Same Basis Sets and Levels of Theory

	T-shaped isomer		linear isomer		$H^{13}C^{13}CH$	
	MP2	BCCD(T)	MP2	BCCD(T)	MP2	BCCD(T)
r_{CH} (Å)	1.0619	1.0643	1.0623[a] 1.0617[b]	1.064[a] 1.064[b]	1.0617	1.0641
r_{CC} (Å)	1.2111	1.2092	1.2110	1.2091	1.2107	1.2090
r_{Mg} (Å)[c]	4.3073	4.3979	3.7615	3.8005		
D_e (cm^{-1})	135	105	101	72		
μ (D)	0.3618	0.3356[d]	0.2772	0.2860[d]		
			Calculated Vibrational Data[e]			
asym CH str	3418.31 (88.75)		3412.71 (174.16)		3419.99 (95.91)	
sym CH str	3499.08 (0.97)		3494.85 (2.24)		3500.98 (0.00)	

[a] Bonded C−H bond. [b] Free C−H bond. [c] Distance to center of CC bond for the T-shaped isomer and the Mg−H distance for the linear isomer. [d] Calculated using the Brueckner reference density (see ref 41). [e] Calculated vibrational frequencies (intensities) in cm^{-1} (km/mol).

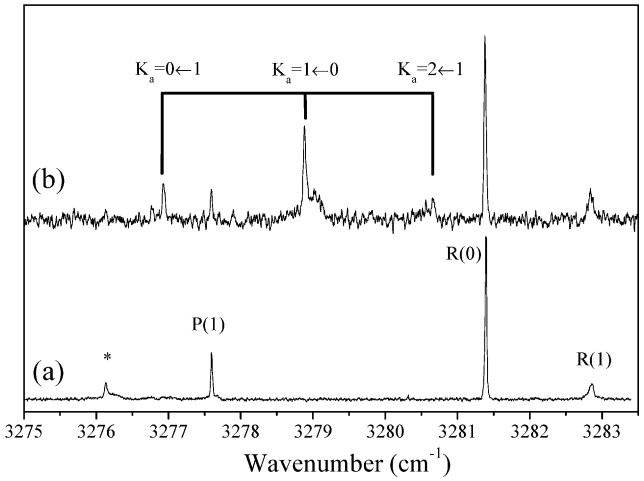

Figure 2. (a) A spectrum of the ν_3 band of $^{13}C_2H_2$ monomer, recorded with the magnesium oven at room temperature. The band marked with an asterisk (*) is assigned to the $^{13}C_2H_2$ dimer, from comparisons with the corresponding gas-phase spectrum (refs 42 and 43). (b) A spectrum obtained with the magnesium oven heated to ~300 °C. The assignments correspond to perpendicular bands of the T-shaped acetylene−Mg binary complex.

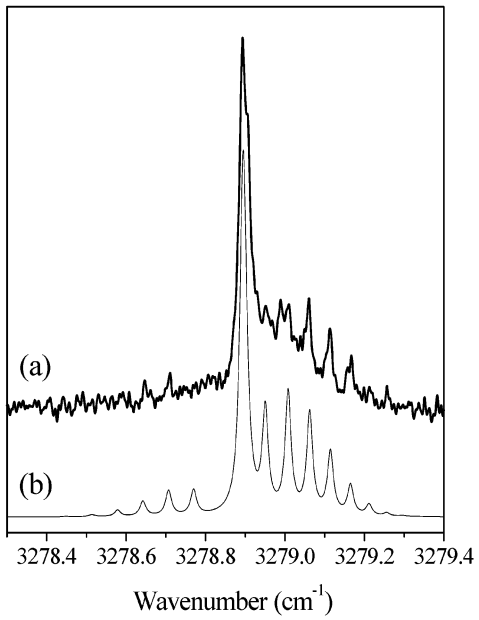

Figure 3. High-resolution scan of the $K_a = 1 \leftarrow 0$ band of the acetylene−Mg binary complex. The smooth curve is a fit to the experimental spectrum using an asymmetric rotor Hamiltonian and the constants listed in Table 2.

assignment. This geometry preserves the rotational symmetry of the acetylene unit, with K_a of the complex correlating with J of free acetylene. As a result, the nuclear spin statistics of the ^{13}C-acetylene (10:6 even:odd J states) carry over to the complex, now being applied to the even and odd K_a states. In fact, the only reason the transitions arising from $K_a = 1$ are observed in the spectrum of such a cold species is that the symmetry prevents the corresponding states from cooling into $K_a = 0$. This preliminary structural assignment is consistent with the more detailed rotational analysis given below.

The most intense band in the spectrum in Figure 2b is tentatively assigned as $K_a = 1 \leftarrow 0$. A high-resolution scan of this region of the spectrum is shown in Figure 3, along with a fitted spectrum based upon a near-prolate asymmetric rotor Hamiltonian. The quantities B', C', $(B'' + C'')/2$, D_J', and D_J'' were varied in the fit and are collected in Table 2. The agreement between the calculated and experimental spectra is quite good, although the line shapes of the low-J transitions are somewhat distorted, as is often the case for species in helium droplets.[28] It is important to note that the natural isotopic abundance of magnesium is 8:1:1 for ^{24}Mg, ^{25}Mg, and ^{26}Mg, so that some of the broadening in the spectrum could result from the three isotopic variations having slightly different rotational constants.

Figure 4 shows all three of the sub-bands from Figure 2, scanned at high resolution. There is clearly significant broadening in the $K_a = 0 \leftarrow 1$ and $K_a = 2 \leftarrow 1$ sub-bands that prevents the observation of some of the fine structure. As a result, a complete set of rotational constants could not be obtained (for example, B'' and C'' could not be determined independently). The fitted values for ν_0, A, and D_K are summarized in Table 2. Including a D_{JK} value of 2.0×10^{-3} cm^{-1} in the fit gave significantly better agreement, particularly for the shapes of the $K_a = 0 \leftarrow 1$ and $K_a = 2 \leftarrow 1$ bands. We have observed large D_{JK} values for other T-shaped acetylene complexes in helium,[29,30] although a detailed physical explanation for this effect

TABLE 2: Experimental Molecular Constants for the Mg−Acetylene Complex[a]

	$v = 0$	$v = 1$		$v = 0$	$v = 1$
A[b]	1.027 (2)	1.027 (2)	D_{JK}[b]	0.0020 (5)	0.0020 (5)
B	0.0306 (3)[c]	0.0326 (3)	D_J	$3.7\ (5) \times 10^{-5}$	$1.2\ (5) \times 10^{-5}$
C	0.0306 (3)[c]	0.0306 (3)	ν_0		3277.9204 (15)
D_K[b]	0.021 (2)	0.021 (2)	μ (D)[b]	0.39 (5)	0.39 (5)

[a] All values are in cm^{-1} unless noted otherwise, and the estimated uncertainties are given in parentheses. [b] The values in the ground and vibrationally excited states were set equal in the fit (see the text). [c] These values correspond to $(B'' + C'')/2$, since B'' and C'' could not be independently determined from the spectrum.

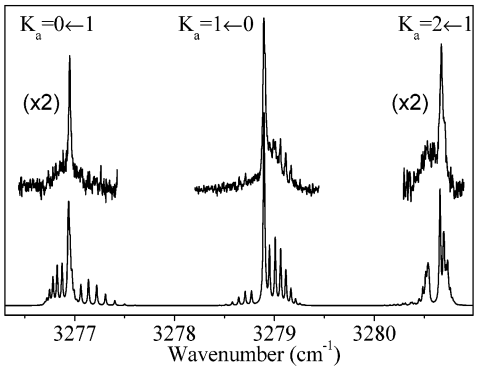

Figure 4. A spectrum showing the entire perpendicular band of the T-shaped acetylene−Mg complex, corresponding to the asymmetric C−H stretch. Three sub-bands are observed and labeled using symmetric top notation. The smooth curve is a fit to the experimental spectrum (fitted constants in Table 2).

is not yet apparent. The fit to the spectrum was done with the constraint that $A'' = A'$, given that three K_a sub-bands provide insufficient data to determine both D_K and ΔA, as noted in our previous paper on acetylene monomer in helium droplets.[21] The assumption that $\Delta A = 0$ makes the determination of D_K somewhat uncertain. Nevertheless, the agreement between the experimental and calculated spectrum is certainly good enough to conclusively assign the spectrum to the T-shaped complex.

The observed frequency shift for the T-shaped complex (relative to the ^{13}C-acetylene monomer in helium (3279.50 cm^{-1} [21]) is 1.58 cm^{-1}, in excellent agreement with the aforementioned calculated redshift of 1.68 cm^{-1}. In addition, the ab initio calculations revealed a second, linear isomer for this system, with a calculated redshift for the asymmetric C−H stretching vibration of 7.28 cm^{-1}. We carried out extensive searches for the spectrum of this isomer, without success. This is in contrast with the HCN−Mg system, where two isomers were observed experimentally.[11] The most likely explanation for why we do not observe the linear isomer is that the barrier between the minima is very low. Indeed, the PES shown in Figure 1 has a barrier that is <10 cm^{-1}, suggesting that the linear isomer cannot be trapped, even under the cold conditions provided by the helium solvent. This barrier is likely even smaller than this estimate once zero point effects are taken into account. We have observed very similar behavior in several other cluster systems grown in helium nanodroplets.[18,31]

Although magnesium and acetylene are both nonpolar, the large polarizability of the magnesium atom can give rise to a significant permanent dipole moment for the binary complex. In particular, the quadrupole−induced-dipole interaction is significant in this system. As noted above, dipole moments for these metal complexes, particularly as a function of metal cluster size, can provide insights into issues such as charge transfer and delocalization. Figure 5 shows two Stark spectra of the $K_a = 1 \leftarrow 0$ sub-band, corresponding to the laser being polarized perpendicular (a) and parallel (b) to the permanent electric field (36.9 kV/cm). As discussed in detail elsewhere,[32] the intensity of the Q branch in a b-type band of a near-prolate asymmetric top is enhanced by the electric field, when the laser polarization is perpendicular to the dc field, while the intensity in this region is reduced to almost zero for parallel polarization.

These Stark spectra were fit using a procedure developed previously,[32] yielding the smooth curves shown in Figure 5. In particular, the Stark energies and wave functions for the ground and excited vibrational states were calculated variationally in the basis set of the free-rotor, asymmetric top wave functions.

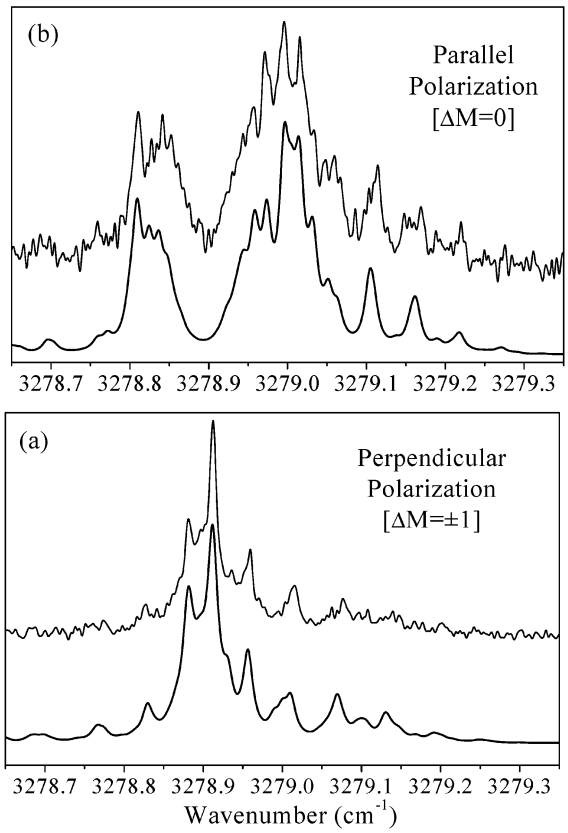

Figure 5. Experimental and fitted Stark spectra of the $K_a = 1 \leftarrow 0$ band of the acetylene−Mg binary complex (36.9 kV/cm applied field), recorded with the laser polarized (a) perpendicular and (b) parallel to the applied field.

The transition dipole moments for the various allowed transitions were then calculated using these wave functions. The calculated spectra are based upon the field free rotational constants from Table 2, with the dipole moment as the only free parameter. The best fits (shown in Figure 5) were obtained with a dipole moment of 0.39 ± 0.05 D (assumed to be the same in the ground and excited vibrational states). It is interesting to note that the dipole moment of the T-shaped Ar−acetylene complex is only 0.026 D.[33] The difference is primarily due to the much larger polarizability of the Mg (10.6 Å^3 [34]), compared to that of argon (1.64 Å^3 [34]), as discussed further below.

The calculated electric dipole moments for the two isomers, at various levels of theory, are also given in Table 1. For the T-shaped isomer, the calculated dipole moments from BCCD-(T) and MP2 theory are 0.336 and 0.362 D, respectively, in good agreement with the experimentally measured value of 0.39 ± 0.5 D. The values for the linear isomer are smaller, namely, 0.286 and 0.277 D, respectively, reflecting the larger distance between the centers-of-mass of the monomers (Table 1).

In our previous work on the HCN−Mg complexes, we made use of difference maps of the electron densities to gain further insights into the nature of the induction interactions giving rise to the dipole moments.[11] These difference density maps are calculated by subtracting a suitably constructed reference density, typically the sum of the noninteracting monomer densities, from the density of the complex. This approach emphasizes the changes in the electron density induced by the formation of the complex. Figure 6a,b shows difference density maps for the T-shaped and linear isomers of Mg−acetylene, respectively. In both cases, the dominant feature is the polarization of the magnesium atom, which shows a clear dipolar

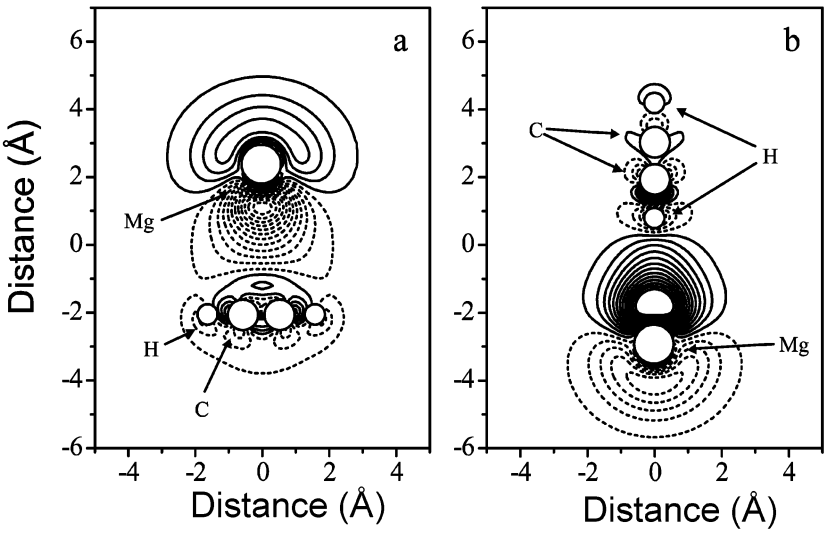

Figure 6. Difference density plots (see the text) for the (a) T-shaped and (b) linear isomers of the acetylene−Mg binary complex. Solid (dashed) contours correspond to regions where there is an increase (decrease) of the electron density due to complex formation. The contours (beginning with the outermost) correspond to densities of $\pm 1.2 \times 10^{-4}$ electrons/Å^3, and the contours proceed inward in steps of $\pm 2.4 \times 10^{-4}$ electrons/Å^3, up to a maximum (minimum) value of $\pm 3 \times 10^{-3}$ electrons/Å^3.

signature, unambiguously identifying the origin of the observed dipole moment. It is interesting to note that the polarization has the opposite sign in the two cases, corresponding to the depletion of charge from between the HCCH and Mg for the T-shaped isomer and the accumulation of charge in the intermolecular region for the linear isomer. This is consistent with the corresponding signs of the angular factors in the expressions for the components of the dipole induced by a linear quadrupole (derived using ref 35), namely,

$$\mu_{\parallel} = \frac{3\Theta_{HCCH}\alpha_{Mg}}{2R^4}(3 - 5\cos^2\theta)\cos\theta$$

$$\mu_{\perp} = \frac{3\Theta_{HCCH}\alpha_{Mg}}{2R^4}(1 - 5\cos^2\theta)\sin\theta \quad (1)$$

where Θ_{HCCH} is the quadrupole moment of acetylene (+7.61 D Å[36]), α_{Mg} is the dipole polarizability of magnesium (10.6 Å^3 [34]), R is the center-of-mass distance, θ is the angle between the intermolecular vector and the molecular axis of the acetylene (0° and 90° for the linear and T-shaped isomers, respectively), and $\mu_{\parallel}$ and $\mu_{\perp}$ are the parallel and perpendicular components of the induced dipole relative to the acetylene molecular axis. Evaluation of these expressions for the T-shaped and linear isomers (using BCCD(T) structural data from Table 1) yields induced dipole moments of 0.319 and −0.267 D, respectively, recovering ∼94% of the corresponding ab initio values.

Results: Larger Mg Clusters

Figure 7 shows a low-resolution scan recorded with the magnesium oven at a higher temperature, optimizing for the pickup of more than one magnesium atom per droplet. The bands near 3274.3 and 3270.5 cm^{-1} grew in more slowly with increasing oven temperature than those already assigned to the binary complex, indicating that more than one Mg atom is required to form the associated complexes. Using the vibrational origin of the $^{13}C_2H_2$ monomer in helium (3279.50 cm^{-1} [21]), we obtain vibrational shifts from the monomer of 5.2 and 9.0 cm^{-1} for the two new bands. While there is little doubt that the less-redshifted band near 3274.3 cm^{-1} is due to a complex with two Mg atoms (see computational results below), the band further to the red is harder to assign. Based on the pattern in the

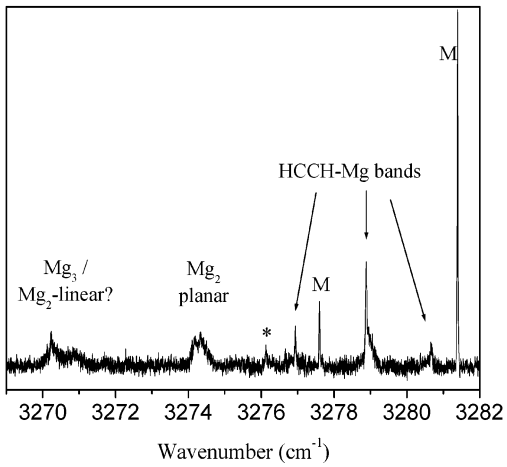

Figure 7. A spectrum recorded at a somewhat higher magnesium oven temperature, resulting in the appearance of bands assigned to acetylene−Mg$_n$ (n = 2, 3) (see the text). The peaks labeled M are the acetylene monomer in helium, and the bands of the binary complex are also indicated. The peak marked with an asterisk (*) is due to the acetylene dimer.

vibrational shifts, it is tempting to assign it to an Mg_3 complex, since this stronger than linear increase in the shift with size is consistent with our previous studies of HCN−Mg$_n$[12] and HCCCN−Mg$_n$,[13] which also show strongly nonadditive interactions. However, our computational results (see below) also found an HCCH−Mg_2 isomer with a predicted vibrational shift matching this band. Therefore the experimental band in question, which does appear to have multiple components, could be due to either of the Mg_2 or Mg_3 complexes, or a mixture of both. We are in the process of improving the pressure calibration of our Mg oven, which should allow us to distinguish between these possibilities based on pickup pressure dependences.

Figure 8 shows a higher resolution scan through the band assigned to the acetylene−Mg_2 cluster. Although there is clearly some structure in the spectrum, the signal levels and resolution are insufficient to determine accurate constants. Nevertheless, by supplementing these experimental results with ab initio calculations, further insights into the nature of this system can be obtained. In particular, geometry optimizations were carried out for the acetylene−Mg_2 complex, along with (MP2) fre-

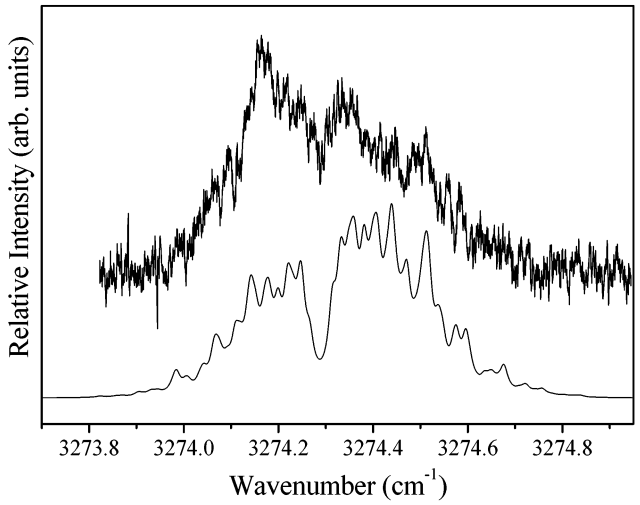

Figure 8. A high-resolution scan through the band assigned to the acetylene−Mg_2 complex. The smooth curve was calculated using rotational constants from the ab initio calculation, modified as discussed in the text to account for the effects of the helium (Table 3).

TABLE 3: Results of Ab Initio Geometry Optimizations and Frequency Calculations (6-311++G(3df,3pd) Basis) for the Two Isomers of the Acetylene−Mg_2 Complex

	planar isomer		crossed isomer	
	MP2	BCCD(T)	MP2	BCCD(T)
r_{CH} (Å)	1.0620	1.0644	1.0621	1.0644
r_{CC} (Å)	1.2119	1.2097	1.2114	1.2093
R (Å)[a]	3.8339	3.9404	3.7836	3.8980
r_{MgMg} (Å)	3.8497	3.8164	4.0054	3.9423
Calculated Vibrational Data[b]				
asym CH str	3416.44 (59.17)		3416.20 (83.37)	
sym CH str	3496.73 (2.27)		3496.73 (2.02)	
Rotational Constants (cm^{-1})				
A	0.0874	0.0888	0.0812	0.0837
B	0.0648	0.0614	0.0628	0.0594
C	0.0372	0.0363	0.0378	0.0370

[a] Center of mass distance between HCCH and Mg_2. [b] Calculated vibrational frequencies (intensities) in cm^{-1} (km/mol).

quency calculations. The minimum energy structure at both levels of theory was found to be a C_{2v} planar geometry, with the HCCH and Mg_2 bond axes parallel to one another. The corresponding structural parameters, vibrational shifts, and rotational constants are collected in Table 3. The calculated vibrational redshift of 3.55 cm^{-1} is in reasonable agreement with the experimental value of 5.2 cm^{-1}, giving us further confidence in the above assignment. The smooth curve in Figure 8 is a computed spectrum generated using the ab initio rotational constants, reduced by a factor of 2.2 (see below) to account for the effects of the helium. Although agreement with experiment is less than satisfactory, the calculated spectrum does reproduce the major features in the experimental spectrum, including the shape of the overall band contour and the "dip" near the vibrational origin. Higher signal level experiments are clearly needed for this system and are being planned.

The planar structure obtained for the acetylene−Mg_2 is somewhat unusual for a weakly bound system, in that it does not place the atoms near the optimal locations based on pairwise interactions. From the PES for the binary complex shown in Figure 1, one would expect the Mg atoms to form a belt around the acetylene molecule, since that allows for the simultaneous optimization of the HCCH−Mg and Mg−Mg pairwise interactions. Indeed, precisely such a structure is predicted to be the minimum for the acetylene−Ar_2 complex.[37] Geometry optimizations for such a configuration (see data in Table 3), with the acetylene and Mg_2 axes in a "crossed" orientation, revealed that it is actually a transition state, with a single imaginary frequency in the torsional coordinate leading to the planar geometry.

TABLE 4: Contribution to Binding Energies (in cm^{-1}) for the Planar and Crossed Isomers of the Acetylene−Mg_2 Complex Calculated at BCCD(t)/6-311++G(3df,3pd) Level

	Planar	Crossed
E_{total}[a]	545.5	502.7
E_{binary}[b]	83.3	109.0
E_{Mg_2}[c]	256.1	273.7
$E_{pairwise}$[d]	422.7	491.7
$E_{3\text{-body}}$[e]	122.8	11.0

[a] Relative to noninteracting HCCH and separated Mg atoms. [b] Binding of single Mg atom to HCCH in equivalent geometry. [c] Binding of Mg_2 relative to Mg atoms in equivalent geometry. [d] $2*E_{binary} + E_{Mg_2}$. [e] $E_{total} - E_{pairwise}$.

Table 4 shows a breakdown of the contributions to the BCCD(T) binding energy of the complex in the two geometries. The total binding energy (E_{total}) relative to separated Mg atoms and HCCH is ∼40 cm^{-1} greater for the planar geometry, however the summed pairwise HCCH−Mg and Mg−Mg interactions are ∼70 cm^{-1} greater for the crossed geometry. Thus there is ∼110 cm^{-1} of additional binding in the planar structure that is due to nominal "three-body" interactions, so-called since they require the presence of both Mg atoms and the HCCH. A significant portion of this can be accounted for by the rather large quadrupole moment of Mg_2 (−1.03 D Å from BCCD(T)/6-311++G(3df,3pd) calculation, which arises from the Pauli repulsion between the Mg atoms. The electrostatic interaction between the two quadrupoles is:

$$E_{q\text{-}q} = \frac{\Theta_{HCCH}\Theta_{Mg}}{4\pi\epsilon_0 R^5} F_{ang} \qquad (2)$$

where R is the center of mass distance (Table 3), and F_{ang} is an angular factor which evaluates to 2.25 or 0.75 in the planar and crossed geometries, respectively.[35] Since the quadrupoles of Mg_2 and HCCH have opposite sign, this interaction is attractive in both geometries, but only accounts for about half of the additional stabilization of the planar structure. Thus there are clearly other 3-body forces at work in the complex, as can be appreciated from the geometric changes in the Mg_2 subunit (Table 3). In the planar geometry, the Mg−Mg distance is 3.82 Å, compared to 4.01 Å in free Mg_2. This contraction of the Mg−Mg bond length results in an increase of ∼40% in the Mg_2 quadrupole, proportionally stregthening the associated interaction. In the crossed Mg_2 isomer, the Mg−Mg distance is 3.94 Å, so the increase in $E_{q\text{-}q}$ is only ∼10%.

In addition to the structural effects discussed above, the large polarizability of Mg means that the non-additivity of induction effects[35] is also important, as can be seen by examining the difference density plots shown in Figure 9a,b for the crossed and planar isomers, respectively. These are computed relative to HCCH and Mg_2, so the effects of the Mg−Mg contraction discussed above are already taken into account. Looking first at the difference density of the crossed structure in Figure 9a, the dipolar polarizations of the individual Mg atoms are quite obvious, reminiscent of the T-shaped isomer of the binary complex (Figure 6a). However, the induced dipoles are in an unfavorable, near-parallel orientation, destabilizing the complex. In the planar isomer, the angular positions of the Mg atoms relative to HCCH (64° and 116°) are such that the perpendicular components of the induced dipoles (eq 1) are essentially zero.

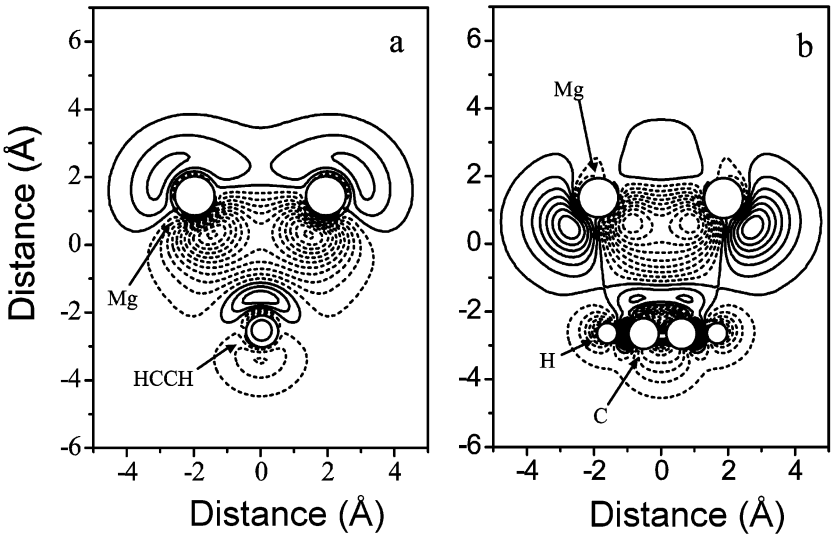

Figure 9. Difference density plots (see the text) for the (a) crossed and (b) planar isomers of the HCCH−Mg_2 complex. Solid (dashed) contours correspond to regions where there is an increase (decrease) of the electron density in the complex relative to the reference systems. The outermost contours correspond to densities of $\pm 1.2 \times 10^{-4}$ electrons/Å^3, and the contours proceed inward in steps of $\pm 2.4 \times 10^{-4}$ electrons/Å^3, up to a maximum (minimum) value of $\pm 3 \times 10^{-3}$ electrons/Å^3.

TABLE 5: Calculated Rotational Constants for the T-Shaped Acetylene−Mg Complex (6-311++G(3df,3pd) Basis)

	MP2	BCCD(T)
A (cm^{-1})	1.1135	1.1149
B (cm^{-1})	0.07031	0.06744
C (cm^{-1})	0.06613	0.06360

So, as can be seen in Figure 9a, the overall effect is to enhance the quadrupolar polarization of the Mg_2, increasing the attractive interaction with the HCCH. However this effect is at least partially balanced by the unfavorable interaction of the anti-parallel induced dipoles on the Mg atoms. A quantitative evaluation of these effects is beyond the scope of this paper, however the qualitative analysis given above illustrates the significance that three-body effects have in determining the structures of weakly bound complexes containing strongly polarizable atoms such as magnesium.

As a final note, we did locate a second minimum on the acetylene−Mg_2 potential energy surface corresponding to a completely linear HCCH−MgMg arrangement of the complex. While this minimum was more weakly bound than the planar complex, having a BCCD(T) [MP2] binding energy of only 99 [116] cm^{-1}, only a small barrier would be required to trap the complex in this geometry in the helium droplets. Therefore, since the calculated (MP2) vibrational shift of this structure is 9.72 cm^{-1}, in good agreement with the unassigned band from the experimental spectrum in Figure 7 (see above), it cannot be ruled out as a possibility. Improvements to the experimental apparatus are currently underway that should allow us to resolve this question in future experiments.

Discussion

Ro-vibrational spectra obtained in helium droplets exhibit a reduction of the rotational constants relative to corresponding gas-phase spectra, due to the tendency of the helium to follow the rotational motion of the molecule or complex.[38,39] Since gas-phase data are unavailable for the acetylene−Mg complex, we must make use of the ab initio rotational constants, listed in Table 5, for these comparisons. For the T-shaped isomer, the ratio of the calculated BCCD(T) [MP2] and experimental ground vibrational state values for $(B + C)/2$ is 2.12 [2.21], which falls within the range (2.5 ± 0.5) typically observed for so-called "heavy" rotational species in liquid helium.[38] In contrast, the A rotational constant of the complex is similar to the B rotational constant of $^{13}C_2H_2$ monomer (0.987 cm^{-1} [21]) and thus falls into the "light molecule" regime, where the helium cannot follow the correspondingly faster motion. The ratio of the calculated and measured A rotational constants for acetylene−Mg is 1.13, in good agreement with the corresponding ratios for other T-shaped acetylene-containing complexes, including acetylene−HCN[30] and acetylene−HF.[29]

It is interesting to note that the B constant for ^{13}C-acetylene in helium is ∼4% smaller than the A constant for the acetylene−Mg complex. This effect can be understood in terms of the intermolecular bending motion, which tends to reduce the moment of inertia about the A-axis. This effect can be quite dramatic, as in the case of acetylene−Ar in the gas phase, where the A constant is 34% larger than the B constant of acetylene.[40] The comparatively small increase for acetylene−Mg (4%) observed here might be the result of the presence of the helium. Indeed, the helium density around the relevant axis is very likely higher for the complex, compared to the acetylene monomer, given that the helium in this region can interact with both the acetylene and the magnesium atom. The result would be a somewhat larger moment of inertia, partially canceling the effects of the intermolecular bending. Unfortunately, the corresponding data for acetylene−Ar in helium are not available, which might otherwise have provided a test of these ideas.

It is evident from Figures 6 and 9 that the distortion of the acetylene charge cloud is more localized than for the Mg atom. However, for the T-shaped isomer the difference density in the region of the C−H bonds is noticeably distorted away from linear. From a molecular orbital point of view, this suggests that the interaction with the magnesium causes an increase in the hybridization of the carbon atoms, albeit a very slight one. Furthermore, we can see from the data in Table 3 that the intensity in the symmetric CH stretch is no longer zero, although it is still only a small fraction of the asymmetric CH stretching intensity. For the acetylene−Mg_2 complex, this effect is less apparent in the difference density (Figure 9), but the calculated intensity for the symmetric CH stretch is even higher than for the binary complex (Table 3). This may indicate the onset of

the rehybridization effects described above for acetylene adsorbed on a copper surface.[6] It would obviously be of considerable interest to see how this effect evolves with further increases in the magnesium cluster size and for other metals.

Summary

High-resolution infrared laser spectroscopy in helium nanodroplets has been used to determine the structure of the acetylene−Mg binary complex to be T-shaped. This is in good agreement with ab initio calculations, which predict this to be the minimum energy structure. Although the ab initio calculations predict the existence of a second, linear isomer, we find no experimental evidence for such a complex. The most likely explanation for this is that the barrier between the two minima on the potential energy surface is too low to isolate the linear complex.

Stark spectroscopy has been used to measure the dipole moment of the T-shaped binary complex, which is again in good agreement with the ab initio calculations. Nevertheless, the experimental dipole moment is considerably larger than that expected from a simple point quadrupole−induced-dipole interaction, which is most likely the result of the highly delocalized nature of the electron cloud associated with the magnesium atom. Difference density plots were presented for the binary complex, that provide further insights into the nature of these induction interactions.

Preliminary results were also presented for complexes containing two and three magnesium atoms, from which the incremental vibrational frequency shifts associated with the asymmetric C−H stretching vibration are obtained. Ab initio calculations on the acetylene−Mg_2 complex indicate that it has a nonslipped parallel structure with C_{2v} symmetry and that this structure results from the competition between two-body and three-body interactions within the complex. Future work will include the extension of these studies to even larger complexes and more reactive metals.

Acknowledgment. Support for this research from the National Science Foundation (CHE-99-87740) and the Air Force Office of Scientific Research (AFOSR) is gratefully acknowledged.

References and Notes

(1) Somorjai, G. A. *Int. Congr. Catal., [Proc.], 8th* **1984**, *1*, I113−I150.
(2) Puddephatt, R. J. *Metal Clusters in Chemistry*; Braunstein, P., Oro, L. A., Raithby, P. R., Eds.; Wiley-VCH: Weinheim, 1998.
(3) Sheppard, N. *Annu. Rev. Phys. Chem.* **1988**, *39*, 589.
(4) Brubaker, M. E.; Trenary, M. *J. Chem. Phys.* **1986**, *85*, 6100.
(5) Ibach, H.; Mills, D. L. *Electron Energy Loss Spectroscopy and Surface Vibrations*; Academic Press: New York, 1982.
(6) Bandy, B. J.; Chesters, M. A.; Pemble, M. E.; McDougall, G. S.; Sheppard, N. *Surf. Sci.* **1984**, *139*, 87.
(7) Marinova, T. S.; Stefanov, P. K. *Surf. Sci.* **1987**, *191*, 66.
(8) Kasai, P. H.; McLeod, D.; Watanabe, T. *J. Am. Chem. Soc.* **1980**, *102*, 179.
(9) Chenier, J. H. B.; Howard, J. A.; Sutcliffe, R. *J. Am. Chem. Soc.* **1983**, *105*, 791.
(10) Nauta, K.; Moore, D. T.; Stiles, P. L.; Miller, R. E. *Science* **2001**, *292*, 481.
(11) Stiles, P. L.; Moore, D. T.; Miller, R. E. *J. Chem. Phys.* **2003**, *118*, 7873.
(12) Stiles, P. L.; Moore, D. T.; Miller, R. E. *J. Chem. Phys.* **2004**, *121*, 3130.
(13) Dong, F.; Miller, R. E. *J. Phys. Chem. A* **2004**, *108*, 2181.
(14) Hartmann, M.; Miller, R. E.; Toennies, J. P.; Vilesov, A. F. *Phys. Rev. Lett.* **1995**, *75*, 1566.
(15) Brink, D. M.; Stringari, S. *Z. Phys. D* **1990**, *15*, 257.
(16) Thompson, C. A.; Andrews, L. *J. Am. Chem. Soc.* **1996**, *118*, 10242.
(17) Nauta, K.; Miller, R. E. *Science* **1999**, *283*, 1895.
(18) Nauta, K.; Miller, R. E. *Science* **2000**, *287*, 293.
(19) Nauta, K.; Miller, R. E. *J. Chem. Phys.* **1999**, *111*, 3426.
(20) Nauta, K.; Miller, R. E. *J. Chem. Phys.* **2001**, *115*, 4508.
(21) Nauta, K.; Miller, R. E. *J. Chem. Phys.* **2001**, *115*, 8384.
(22) Huang, Z. S.; Jucks, K. W.; Miller, R. E. *J. Chem. Phys.* **1986**, *85*, 3338.
(23) Boys, S. F.; Bernardi, F. *Mol. Phys.* **1970**, *19* (4), 553.
(24) Hesselmann, A.; Jansen, G. *J. Chem. Phys.* **2000**, *112*, 6949.
(25) Abramowitz, M.; Stegun, I. A. *Handbook of Mathematical Functions*; Dover Publications, Inc.: New York, 1972.
(26) Hirshfeld, F. L. *Theor. Chim. Acta* **1977**, *44*, 129.
(27) Werner, H. J.; Knowles, P. J.; Almlof, J.; Amos, R. D.; Berning, A.; Deegan, M. J. O.; Eckert, F.; Elbert, S. T.; Hampel, C.; Lindh, R.; Meyer, W.; Nicklass, A.; Peterson, K.; Pitzer, R.; Stone, A. J.; Taylor, P. R.; Mura, M. E.; Pulay, P.; Scheutz, M.; Stoll, H.; Thorsteinsson, T.; Cooper, D. L. *MOLPRO, a package of ab initio programs*; Birmingham, U.K., 2002.
(28) Callegari, C.; Reinhard, I.; Lehmann, K. K.; Scoles, G.; Nauta, K.; Miller, R. E. *J. Chem. Phys.* **2000**, *113*, 4636.
(29) Douberly, G. E.; Nauta, B. K.; Miller, R. E. *Chem. Phys. Lett.* **2003**, *377*, 384.
(30) Nauta, K.; Miller, R. E. *Chem. Phys. Lett.* **2001**, *346*, 129.
(31) Douberly, G. E.; Miller, R. E. *J. Phys. Chem. B* **2003**, *107*, 4500.
(32) Moore, D. T.; Oudejans, L.; Miller, R. E. *J. Chem. Phys.* **1999**, *110*, 197.
(33) DeLeon, R. L.; Muenter, J. S. *J. Chem. Phys.* **1980**, *72*, 6020.
(34) Lide, D. R.*CRC Handbook of Chemistry and Physics*, 71st ed.; CRC Press: Boca Raton, FL, 1990.
(35) Stone, A. J. *The Theory of Intermolecular Forces*; Oxford University Press: Oxford, 1996.
(36) Kling, H.; Geschka, H.; Huttner, W. *Chem. Phys. Lett.* **1983**, *96*, 631.
(37) Hasse, R. D.; Severson, M. W.; Szczesniak, M. M.; Chalasinski, G.; Cieplak, P.; Kendall, R. A.; Cybulski, S. M. *J. Mol. Struct.* **1997**, *436*−*437*, 387.
(38) Callegari, C.; Conjusteau, A.; Reinhard, I.; Lehmann, K. K.; Scoles, G. In *Rovibrational Bound States in Polyatomic Molecules*; Law, M. M., Atkinson, I. A., Hutson, J. M., Eds.; CCP6: Daresbury, U.K., 1999.
(39) Kwon, Y.; Huang, P.; Patel, M. V.; Blume, D.; Whaley, K. B. *J. Chem. Phys.* **2000**, *113*, 6469.
(40) Hu, T. A.; Prichard, D. G.; Sun, L. H.; Muenter, J. S.; Howard, B. J. *J. Mol. Spectrosc.* **1992**, *153*, 486.
(41) Hesselmann, A.; Jansen, G. *Chem. Phys. Lett.* **1999**, *315*, 248.
(42) Miller, R. E.; Vohralik, P. F.; Watts, R. O. *J. Chem. Phys.* **1984**, *80*, 5453.
(43) Fraser, G. T.; Suenram, R. D.; Lovas, F. J.; Pine, A. S.; Hougen, J. T.; Lafferty, W. J.; Muenter, J. S. *J. Chem. Phys.* **1988**, *89*, 6028.